Holstein polaron

J. Bonča

FMF, University of Ljubljana and J. Stefan Institute, 1000, Slovenia

S. A. Trugman

Theory Division, Los Alamos National Laboratory, Los Alamos, New Mexico 87545

I. Batistić

Institute of Physics of the University, HR-1000, Zagreb, Croatia

We describe a variational method to solve the Holstein model for an electron coupled to dynamical, quantum phonons on an infinite lattice. The variational space can be systematically expanded to achieve high accuracy with modest computational resources (12-digit accuracy for the one-dimensional polaron energy at intermediate coupling). We compute ground-state and low-lying excited-state properties of the model at continuous values of the wave vector k in essentially all parameter regimes. Our results for the polaron energy band, effective mass, and correlation functions compare favorably with those of other numerical techniques, including the density-matrix renormalization-group technique, the global-local method, and the exact diagonalization technique. We find a phase transition for the first excited state between a bound and unbound system of a polaron and an additional phonon excitation. The phase transition is also treated in strong-coupling perturbation theory. [S0163-1829(99)08327-7]

I. INTRODUCTION

Polaron formation as a consequence of electron-phonon coupling appears in many contexts in condensed-matter physics, including charge carriers in colossal magnetoresistance materials[1,2] and in high-temperature superconductors.[3,4] As theoretical research in this field spans over five decades, many analytical techniques have been applied to this problem.[5] The applicability of these methods is usually limited to a particular parameter regime, frequently far from the physically most interesting crossover regime. Despite extensive analytical work in this field, there remain many open problems, including the nature of the crossover to large polaron mass, the form of various correlation functions, the nature of the polaron excited states, and dynamic properties of the polaron.

Constantly growing computer capabilities have allowed research in this field to take advantage of various numerical methods, including exact diagonalization techniques (ED),[6–12] quantum Monte Carlo calculations (QMC),[13,14] variational methods including the global-local method (GL),[15,16] and recently developed density-matrix renormalization-group techniques (DMRG).[17] A comparison of results obtained by different methods for energy bands and effective masses is contained in the work of Romero *et al.*[15] Although most of these methods give reliable results in a wide range of parameter regimes, each suffers from different shortcomings. The ED technique gives reliable results on small lattices (up to 20 sites[8]) for ground- and excited-state properties. Results are limited to discrete momentum k points. QMC methods can treat large system sizes (over 1000 lattice sites) and provide accurate results for thermodynamic polaron properties. Dynamic properties, however, require analytic continuation from imaginary time, which is an ill-posed problem that is extremely sensitive to

statistical noise. The GL method gives reliable results for energy bands and the polaron effective mass on reasonably large system sizes (32 sites); however, it is limited to ground-state properties. The DMRG method seems to be most successful in computing ground-state properties, including various correlation functions. Despite the lack of translational symmetry, it provides reasonably accurate results for energy bands and the effective mass. It can deal with large system sizes (e.g., 80 sites and 30 phonons per site), delivering reliable results in essentially all regimes from weak to strong coupling. In the weak-coupling regime, finite-size effects, enhanced by the open boundary conditions, may become important. It generally treats large systems with open boundary conditions and does not allow the calculation of dynamic or large-k properties or excited states, although there are some exceptions to these rules.[18]

In this paper we focus on several issues of the Holstein problem. We present a simple and computationally efficient method based on the exact diagonalization technique. We apply the method to the one-dimensional, single-electron Holstein model. Among the advantages of our method are the simplicity of our approach, the efficiency in selecting the variational space, and the ability to compute both ground- and excited-state physical properties of the system at continuous total wave vector k. We define the variational space on an infinite lattice. Even though most of our calculations were done on a workstation, our results are often superior to those of other numerically more intensive methods.[8,9,17] We test the method by comparing results for the energy band, effective mass, quasiparticle weight, and correlation functions with some of the most successful recent numerical methods.

The second part of this paper is devoted to the investigation of the first excited state of the model. Using our numerical method as well as a strong-coupling analytical approach,

we find a phase transition between a state where the polaron forms a bound state with an additional phonon excitation, and one where there is no bound state.

Generalizations of this method can even be used to calculate coherent quantum dynamics far from equilibrium, including those of a polaron driven by a strong electric field,[19] and of an electron tunneling across a potential drop while coupled to phonons.[20]

We consider the Holstein Hamiltonian[21]

$$H = -t \sum_j (c_j^\dagger c_{j+1} + \text{H.c.}) - \lambda \sum_j c_j^\dagger c_j (a_j + a_j^\dagger)$$

$$+ \omega \sum_j a_j^\dagger a_j, \tag{1}$$

where $c_j^\dagger$ creates an electron and $a_j^\dagger$ creates a phonon on site j. We consider the case where a single electron hops between nearest-neighbor Wannier orbitals in one dimension (1D), and interacts with dispersionless optical phonons. The electron-phonon coupling strength is λ, and is local in real space (k independent). The parameters $t, \omega,$ and λ all have units of energy, and can be used to form two dimensionless ratios. (Different conventions for the parameters are sometimes used in other papers.)

It is clear at the outset that for any finite values of the parameters, the exact ground state will be a delocalized state with momentum $\vec{k}$, and not a ''self-trapped'' solution that breaks translation invariance. The simple argument is that if the ground state were self-trapped, its center could be shifted and a degenerate ground state obtained. If the Hamiltonian has any nonzero matrix element between states with different centers, a lower energy state can be obtained by a phased superposition of wave functions with different centers (a Bloch state). The only known way that this argument can fail is with (unphysically) strong electron-phonon coupling as $\omega \to 0$ to a gapless phonon spectrum, in which case the matrix element between different centers can vanish.[22] In that case, an exact ground state can be written as either self-trapped or as a Bloch state. Self-trapping cannot occur here because the phonon spectrum has a gap. Although the exact ground state is a Bloch state, for some parameters (e.g., very large λ), a self-trapped solution can have a low variational energy.[23] It has indeed been proven that polaron ground-state properties, including the energy and effective mass, are analytic functions of the Hamiltonian parameters.[24] We will see below that such a theorem cannot be extended to include excited states.

II. THE METHOD

A complete set of basis states for the many-body Hilbert space can be written

$$|M\rangle = |j; \ldots, n_{j-1}, n_j, n_{j+1}, \ldots \rangle, \tag{2}$$

where j is the electron site and there are n_m phonons on site m. A variational subspace is constructed beginning with an initial state, taken to be an electron on site $j=0$ with no phonons, and operating repeatedly (N_h times) with the off-diagonal pieces of the Hamiltonian, Eq. (1). At each step, a basis state is added when there is a nonzero t or λ matrix
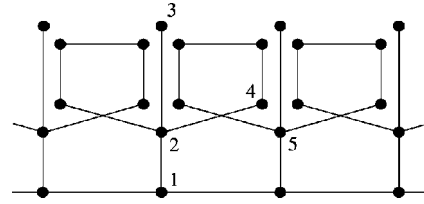

FIG. 1. Small variational Hilbert space shown for the polaron is a subset of the $N_h = 3$ space. Basis states in the many-body Hilbert space are represented by dots, and nonzero off-diagonal matrix elements by lines. The x coordinate of the dots is (aside from small displacements) the coordinate of the electron. Vertical bonds create phonons, and horizontal or nearly horizontal bonds are electron hops. State $|1\rangle$ is an electron on site 0 and no phonons. State $|2\rangle$ is an electron and phonon, both on site 0. State $|4\rangle$ is an electron on site 1 and a phonon on site 0, which is reached from state $|2\rangle$ by hopping the electron to the right. State $|5\rangle$ is a translation of state $|2\rangle$. The Hamiltonian is sparse in this basis, with at most four bonds attached to a dot. The dots can also be thought of as Wannier orbitals in a one-body periodic tight-binding model.

element to a state previously in the space. These states and all of their translations on an infinite lattice are included in the variational space. (A translation moves the electron and all phonon excitations m sites to the right.) If a basis state can be generated in more than one way, only one copy is retained. All nonzero matrix elements of the Hamiltonian between retained basis states are included (some of this construction appears in Ref. 26).

A small variational Hilbert space is shown in Fig. 1. The dots may be thought of as basis states in the many-body Hilbert space, or alternatively as Wannier orbitals in a periodic (one-body) tight-binding model, with hopping matrix elements given by the bonds. The variational space shown in Fig. 1 is still infinite, since the lattice repeats periodically to infinity. It is clear from Bloch's theorem, however, that each eigenstate can be written as $e^{ikj}\Psi_m$, where k is the momentum, j is the unit cell, and Ψ_m is a set of M complex amplitudes, one for each state in the unit cell ($M=7$ for the example of Fig. 1). For a given momentum k, the resulting numerical problem is to find the eigenstates of an $M \times M$ (sparse) Hermitian matrix using Lanczos or another method.

Figure 2 plots the energy eigenvalues for a larger variational space containing a maximum of nine phonon excitations. The figure superficially resembles a ''band structure,'' which, however, encodes ground- and excited-state information for the many-body (many phonon) polaron problem. The ac conductivity of the polaron, for example, appears as an ''interband'' transition in this mapping.

The largest variational basis that we have used has $N_h = 22$ or $M = 1.2 \times 10^7$ states. It is usually unnecessary to use such a large basis for intermediate-coupling ground-state properties, even to obtain 12-digit accuracy for the energy. The variational Hilbert space we construct is not a standard one, and appears to add basis states more efficiently than some other methods. A basis state is included if it can be reached using N_λ phonon creation operators and N_t electron hops in any order with $N_t + N_\lambda \leq N_h$. For a given N_h, there is a basis state with N_h phonon quanta on the same site as the electron and no phonon excitations elsewhere. There is also a basis state with $N_h - 1$ quanta on the site adjacent to the
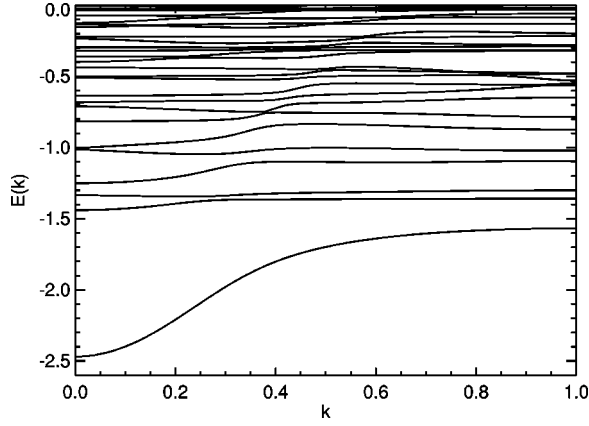
FIG. 2. Ground- and excited-state energy eigenvalues (those $E_j \lesssim 0$) are plotted as a function of k (in units of π) for $\lambda = \omega = 1$, $N_h = 9$, $M = 1185$. Excited states consist of the polaron with additional bound or unbound phonon excitations. The hopping parameter $t = 1$ is assumed here and throughout this work wherever t is not explicitly specified.

FIG. 3. Polaron energy as a function of k (in units of π). Lines represent our results for two different sets of parameters obtained by calculating $E(k)$ at 100 k points. Circles, squares, and diamonds are results obtained with global-local (Ref. 15), DMRG (Refs. 15 and 17), and ED (Ref. 8) calculations, respectively.

electron and no phonon excitations elsewhere. For N_h odd, there is a basis state with $(N_h - 1)/2$ quanta on the electron site and an equal number simultaneously on a first-neighbor site. The maximum distance that a phonon excitation can appear from the electron is $l = N_h - 1$, but then only a single quantum and only if there are no phonons excited elsewhere in the system.[25] Only the basis states from a single unit cell (a single-electron position) are stored in computer memory.

The energy of a polaron for a finite chain of N sites with periodic boundary conditions is *lower* than that for an infinite lattice with the same parameters. (This is easy to verify in weak-coupling perturbation theory, or numerically.) Thus, previous exact diagonalization and most other variational approaches produce energies that are variational for the particular lattice size N that they treat, but are not variational in the thermodynamic limit $N \to \infty$. The energy we calculate is, in contrast, variational in the thermodynamic limit. (The quoted DMRG energies are extrapolated and not variational, although they are generally rather accurate.)

Having the capability to compute the polaron energy $E(k)$ at any k rather than being limited to multiples of $2\pi/N$ makes our method more accurate for computing the effective mass of the polaron using the standard formula

$$\frac{m_0}{m^*} = \frac{1}{2t} \left. \frac{\partial^2 E(k)}{\partial k^2} \right|_{k=0}, \qquad (3)$$

where $m_0 = 1/(2t)$ is the effective mass of a free electron. The second derivative is evaluated by small finite differences in the neighborhood of $k = 0$. Note that although the calculated energy $E(k)$ is a variational bound for the exact energy, there is no such control on the mass, which may be either above or below the exact answer, and is expected to be more difficult to obtain accurately. Nevertheless, in the intermediate-coupling regime where our method at $N_h = 20$ gives an energy accuracy of 12 decimal places, one can calculate the effective mass extremely accurately (6–8 decimal places) by letting $\Delta k \to 0$.
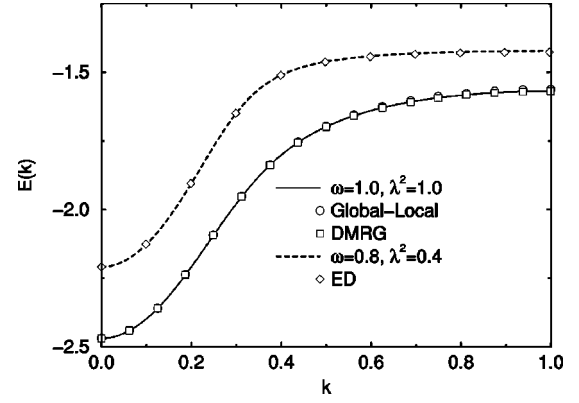
Further information about the quasiparticle may be obtained by computing the quasiparticle residue, the overlap (squared) between a bare electron and a polaron,

$$Z_k = |\langle \psi_k | c_k^\dagger | 0 \rangle|^2, \qquad (4)$$

where $|0\rangle$ is the state with no electron and no phonon excitations, and $|\psi_k\rangle$ is the polaron wave function at momentum k. The numerical results for $Z_{k=0}$ given in Sec. III differ by less than 1% from results for the reciprocal effective mass m_0/m^* obtained from Eq. (3). At finite k, Z_k provides information about the electronic character of the polaronic state. The phonon contribution to the quasiparticle can be measured by the k dependent mean phonon number

$$N_k^{ph} = \sum_i |\langle \psi_k | a_i^\dagger a_i | \psi_k \rangle|^2. \qquad (5)$$

To describe the polaron at different k we have also computed the static correlation function between the electron position and the oscillator displacement

$$\chi(i-j) = \langle \psi_k | c_i^\dagger c_i (a_j + a_j^\dagger) | \psi_k \rangle, \qquad (6)$$

and the distribution of the number of excited phonons in the vicinity of the electron

$$\gamma(i-j) = \langle \psi_k | c_i^\dagger c_i a_j^\dagger a_j | \psi_k \rangle. \qquad (7)$$

III. GROUND-STATE RESULTS

In this section we compare our results for the ground-state properties of the Holstein model to those obtained by other numerical methods. We also calculate polaron correlation functions at finite values of the Bloch wave vector k.

We start by comparing energy bands $E(k)$ for two different sets of parameters. Figure 3 compares the present method to the DMRG,[15,17] GL,[15] and the finite cluster ED technique.[8] Using $N_h = 20$ we achieve an accuracy in the thermodynamic limit of 12 decimal places for small k and at least four decimal places for large k. Our results for $E(k)$ are presented as continuous curves. Agreement of our results with DMRG and ED is good; however, there is a slight disagreement with

TABLE I. A comparison of the polaron ground-state energy at $k=0$ for two different parameter sets.

λ/ω	Present	ED $N=16$	DMRG $N=32$	Global local
1	-2.469684723933	-2.46968477	-2.46968	-2.46931
$\sqrt{2}$	-2.998828186867	-2.99882816	-2.99883	-2.99802

the global-local method at larger k, which also disagrees with the DMRG method. There is also a slight disagreement with the ED at larger k which we attribute to the smaller system size used in finite cluster ED calculations. As we will demonstrate later in this paper, the extent of the lattice deformation (the size of the polaron) increases as k approaches the Brillouin-zone boundary, which makes finite-cluster calculations more susceptible to finite-size effects.

In Table I we compare the polaron ground-state energy at $k=0$ for two different parameter sets obtained by our and three other numerical methods, exact diagonalization (ED),[28] DMRG,[17] and global-local variational.[15] Comparisons with a greater variety of methods can be found in Romero et al.[15] We have limited our comparison to those methods that are accurate to at least four decimal places. Our method converges to all of the digits shown using $N_h=15$ or $M=88\,052$ basis states for $\lambda=\omega=1$, and $N_h=18$ or $M=731\,027$ basis states for $\lambda=\sqrt{2}, \omega=1$. The ground-state energy converges exponentially with N_h, with the accuracy improving by approximately one order of magnitude as N_h is increased by 1. This exponential convergence is used to estimate the error. The larger ($N_h=18$) calculation runs in under a minute on a modest workstation.

Figure 4 shows our results for the effective mass Eq. (3) computed with $N_h=20$ in comparison with GL and DMRG methods. The parameters span different physical regimes including weak and strong coupling (respectively, small and large λ/ω), and adiabatic ($\omega/t \ll 1$) and antiadiabatic ($\omega/t \gg 1$) regimes. We find good agreement with GL away from strong coupling and good agreement in all regimes with DMRG. DMRG calculations are not based on finite-k calculations due to a lack of periodic boundary conditions, so they extrapolate the effective mass from the ground-state data using chains of different sizes, which leads to larger error bars and more computational effort. Notice that their discrete data
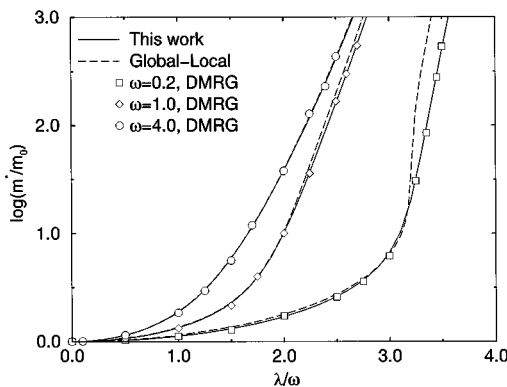
are slightly scattered around our curves. Nevertheless, both methods agree well. We have compared our results for effective mass obtained on different systems from $N_h=16$ with $M=178\,617$ states to $N_h=20$ with $M=2\,975\,104$ states and obtained convergence of results to at least four decimal places in all parameter regimes presented in Fig. 4. Our error is therefore well below the linewidth. Even though there is no phase transition in the ground state of the model, the polaron becomes extremely heavy in the strong-coupling regime. The crossover to a regime of large polaron mass is more rapid in adiabatic regime (smaller ω/t).

Figure 5 shows the quasiparticle residue Z_k and the mean phonon number N_k^{ph} as a function of k for the case of small $\lambda_0 \equiv \lambda^2/2\omega t$ ($\lambda^2=0.4$, $\omega=0.8$) and large λ_0 ($\lambda^2=3.2$, $\omega=0.8$). The two sets of parameters correspond to the large and small polaron regime, respectively.[9] The DMRG cannot straightforwardly compute this quantity, and we compare our results with cluster calculations. Open symbols represent the results of Wellein and Fehske[8] obtained on a $N=14$ site cluster for the same choice of parameters. Except for the fact that their results are limited to discrete k points defined by the size of their system, we find excellent agreement between the two methods in the weak-coupling case. In the strong-coupling regime there is an approximately 1% disagreement in N_k^{ph} due to a lack of phonon degrees of freedom in the variational space of the ED calculation. Our results in the weak-coupling case show a smooth crossover from predominantly electronic character of the wave function for small k (large Z_k and small $N_k^{ph} \approx 0$) to predominantly phonon character around $k=\pi$ characterized by $Z_k \approx 0$ and $N_k^{ph} \approx 1$. In the strong-coupling regime there is less k dependence. The Z_k is already close to zero at small k, indicating strong electron-phonon interactions that lead to a large polaron mass.
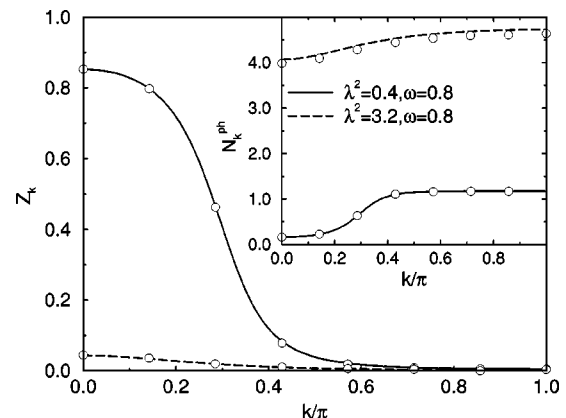
Jeckelmann and White have calculated the electron-

FIG. 4. Logarithm of the effective mass m^*/m_0 as a function of λ/ω. Our results are plotted as full lines, and global-local results as dashed lines (Ref. 15). Open symbols, indicating the value of ω, are DMRG results (Ref. 17).

FIG. 5. Quasiparticle weight Z_k and in the inset the total number of phonons N_k^{ph} as a function of the wave vector k. Results by Wellein and Fehske (Ref. 8) are represented by open circles.
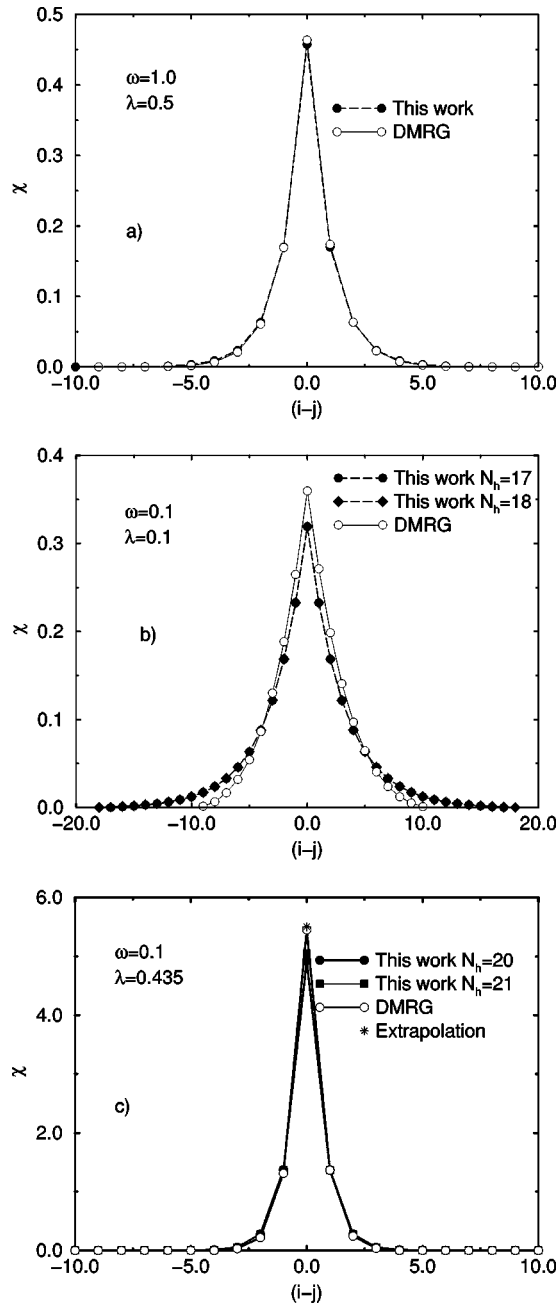
FIG. 7. Lattice deformation χ as a function of $(i-j)$ for $\omega = 0.8$, $\lambda^2 = 0.4$, and $N_h = 18$, for four different values of momentum k. The variational Hilbert space for $N_h = 18$ allows nonzero correlations to a maximum distance $|i-j|_{max} = 17$. Only distances up to 15 are plotted.

$\chi(l) \neq \chi(-l)$. In this parameter regime our results have fully converged, as we can see from the perfect overlap of results of systems with two different sizes of the Hilbert space $N_h = 17, 18$. Figure 6(c) plots correlations for $\omega = 0.1$ and $\lambda = 0.435$, which belongs to the strong-coupling, small polaron regime. The DMRG produces superior results in this regime, where our calculation at $N_h = 21$ has not fully converged to the large N_h limit. Our results are, nevertheless, in qualitative agreement with the DMRG. We conclude that both techniques give reliable results in the intermediate-coupling regime, and that they complement each other in the weak- and strong-coupling regimes.

A thorough investigation of correlation functions using ED and the variational Lanczos method was performed by Wellein and Fehske.[9] Although we do not show a direct comparison with their work, our results for correlation functions agree qualitatively with their calculations.

While the strength of the DMRG calculation is exhibited in its ability to compute ground-state properties of large systems, it is limited in its computation of excited states. In Fig. 5 we have shown how the nature of the polaron transforms from predominantly electronic character at $k = 0$ to phononic around $k = \pi$. We follow this transformation by computing the correlation function χ for four different values of k, shown in Fig. 7. These parameters correspond to the weak-coupling case in Fig. 5. At $k = 0$, where the group velocity is zero, the deformation is limited to only a few lattice sites around the electron. It is always positive and exponentially decaying. At finite but small $k = \pi/4$, the deformation around the electron increases in amplitude and rings (oscillates in sign) as the polaron acquires a finite group velocity. At $k = \pi/2$ the ringing is strongly enhanced. Note also that the spatial extent of the deformation increases in comparison to $k = 0$. The range of the deformation is maximum at $k = \pi$, where it extends over the entire region shown in the figure. In keeping with the larger extent of the lattice deformation near $k = \pi$, the ground-state energy $E(\pi)$ converges more slowly with the size of the Hilbert space.

We have also computed χ for the strong-coupling case $\omega = 0.8$, $\lambda^2 = 3.2$ (not shown). We find only weak k depen-

FIG. 6. Lattice deformation χ as a function of $(i-j)$ for (a) $\omega = 1.0$ and $\lambda = 0.5$, (b) $\omega = 0.1$ and $\lambda = 0.1$, and (c) $\omega = 0.1$ and $\lambda = 0.435$. Our results are represented by filled symbols and those of Jeckelmann and White (Ref. 17) by open circles. In case (c) our results for $N_h = 21$ have not yet reached the large N_h limit. The star represents an extrapolation of our data (assuming exponential convergence) to $N_h \to \infty$, $\chi(0) = 5.5 \pm 0.1$.

phonon correlations at $k = 0$ for the 1D and 2D polaron using the DMRG method.[17] We compare our results with theirs for the 1D case. There is good agreement in Fig. 6(a) for intermediate-coupling parameters $\omega = 1$ and $\lambda = 0.5$. Figure 6(b) plots correlations for $\omega = 0.1$ and $\lambda = 0.1$, which corresponds to weak coupling in the adiabatic limit. In this regime the DMRG method gives less reliable results. The size of the polaron is underestimated, possibly due to finite-size effects in open boundary conditions. Note also that the DMRG method does not give symmetric results as it should, i.e.,
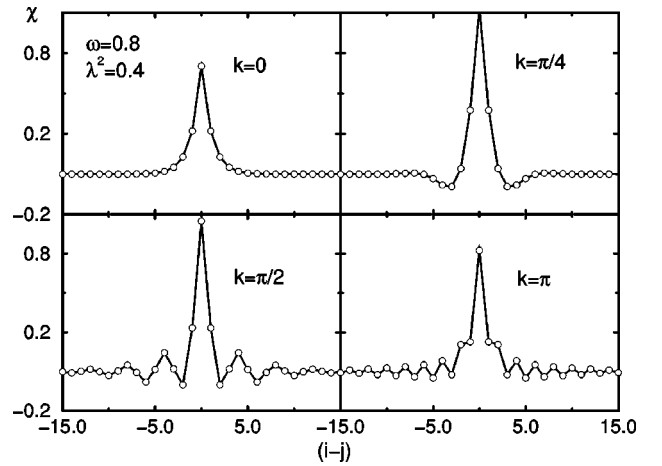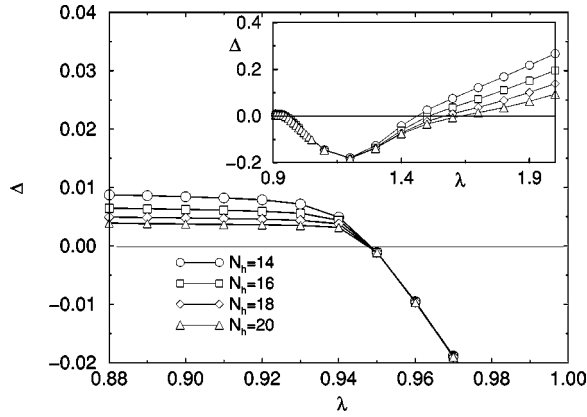
FIG. 8. First excited-state binding energy $\Delta = E_1 - E_0 - \omega$ as a function of λ. Results are for $\omega = 0.5$ and various Hilbert space sizes N_h. Inset: binding energy over a wider range of λ.
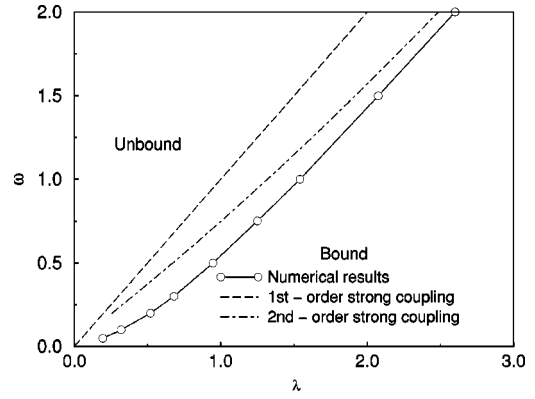

FIG. 9. Phase diagram for the bound to unbound transition of the first excited state, obtained using the condition $\Delta(\omega, \lambda) = 0$. The corresponding phase diagram for the ground state would be blank— there is no phase transition in the ground state, only a crossover.

dence, which is a consequence of the crossover to the small polaron regime. The lattice deformation is localized predominantly on the electron site.

IV. WHAT IS THE NATURE OF THE FIRST EXCITED STATE?

In this section we focus on the question of whether an extra phonon excitation forms a bound state with the polaron, or instead remains as two widely separated entities. Using numerical and analytical approaches we will show that there exists a sharp phase transition between these two states. Although the ground-state energy E_0 is an analytic function of the parameters in the Hamiltonian, there are points at which the energy E_1 of the first excited state is nonanalytic. In previous work, Gogolin has found bound states of the polaron and additional phonon(s), but he does not obtain a phase transition between bound and unbound states because his approximations are limited to strong coupling $\lambda/\omega \gg 1$.[27] A phase transition between a bound and unbound first excited state has been calculated for dimension $d = 3$ using a dynamical coherent potential approximation[29] (CPA) and dynamical mean-field theory.[30]

A. Numerical results

We begin by computing the energy difference $\Delta E = E_1 - E_0$, where E_1 and E_0 are the first-excited-state and the ground-state energies at $k = 0$ (the two lowest bands in Fig. 2). In the case where the first excited state of a polaron can be described as a polaron ground state and an unbound extra phonon excitation, this energy difference should in the thermodynamic limit equal the phonon frequency, $\Delta E = \omega$. In Fig. 8 we plot the binding energy $\Delta = \Delta E - \omega$ for $\omega = 0.5$ as a function of the electron-phonon coupling λ for various sizes of the variational space. We see two distinct regimes. Below $\lambda_c \sim 0.95$, Δ varies with the system size but remains positive ($\Delta > 0$). Physically, for $\lambda < \lambda_c$, the additional phonon excitation would prefer to be infinitely separated from the polaron, but is confined to a distance no greater than $N_h - 1$ by the variational Hilbert space. As the system size increases, Δ slowly approaches zero from above as the "particle in a box" confinement energy decreases. In the other

regime, $\lambda > \lambda_c$, our data have clearly converged and $\Delta < 0$. This is the regime where the extra phonon excitation is absorbed by the polaron forming an excited bound polaron. Since the excited polaron forms an exponentially decaying bound state, the method already converges at $N_h = 14$. In the inset of Fig. 8 we show the binding energy Δ in a larger interval of electron-phonon coupling λ. Although the results cease to converge at larger λ, we notice that the binding energy Δ reaches a minimum as a function of λ. As we will demonstrate within the strong-coupling approximation, the true binding energy approaches zero exponentially from below with increasing λ. In Fig. 9 we show the phase diagram, valid for $k = 0$, separating the two regimes. The phase boundary, given by $\Delta = 0$, was obtained numerically and using strong-coupling perturbation theory in t to first and second
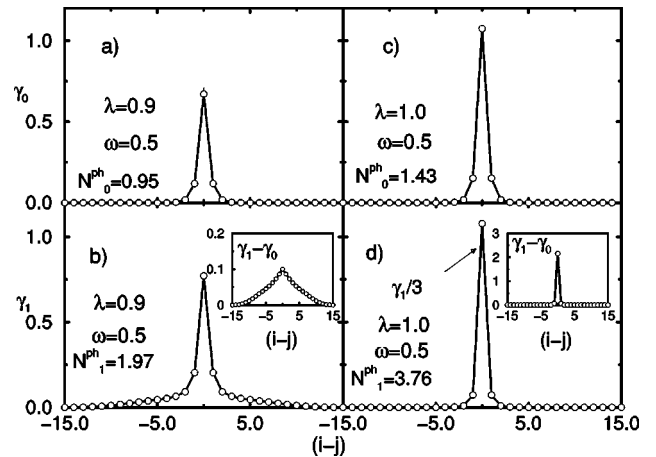

FIG. 10. Phonon number γ as a function of the distance from the electron position $(i - j)$ for the ground state (a) and the first excited state (b) both computed at $\lambda = 0.9$ and the same in (c) and (d) for $\lambda = 1.0$. All data are computed at phonon frequency $\omega = 0.5$ and $N_h = 18$. Note that (d) is a plot of $\gamma_1/3$. Insets in (b) and (d) represent differences $\gamma_1 - \gamma_0$ as a function of the distance $(i - j)$. In (b), $\gamma_1 - \gamma_0$ drops to zero around $|i - j| = 15$. This is a finite-size effect. Computing the same quantity with larger N_h below the phase transition would lead to a larger extent of the correlation function indicating that the extra phonon excitation is not bound to the polaron.

order. Details of the latter calculation are given in Sec. IV B. The phase transition where Δ becomes negative at sufficiently large λ is also seen in exact diagonalization calculations.[31]

In Fig. 10 we compute the distribution of the number of excited phonons in the vicinity of the electron $\gamma(i-j)$, Eq. (7), for the ground state γ_0 and the first excited state γ_1 slightly below ($\lambda=0.9$), and above ($\lambda=1.0$) the transition for $\omega=0.5$. The central peak of the correlation function γ_1 below the transition point is comparable in magnitude to γ_0 [Figs. 10(a) and 10(b)]. The main difference between the two curves is the long-range decay of γ_1 as a function of distance from the electron, onto which the central peak is superimposed. The extra phonon that is represented by this long-range tail extends throughout the whole system and is not bound to the polaron. See also the difference $\gamma_1 - \gamma_0$ in the inset of Fig. 10(b). The existence of an unbound, free phonon is confirmed by computing the difference of the total phonon number $N_{0,1}^{ph}=\Sigma_l \gamma_{0,1}(l)$. This difference should equal one below the transition point. Our numerical values give $N_1^{ph} - N_0^{ph} \sim 1.02$. We attribute the deviation from the exact result to finite-size effects.

Correlation functions above the transition point [Figs. 10(c) and 10(d)] are physically different. First, phonon correlations in γ_1 decay exponentially, which also explains why the convergence in this region is excellent. Second, the size of the central peak in γ_1 is three times higher than γ_0. [Note that to match scales in Fig. 10(d) we divided γ_1 by 3.] The difference in total phonon number gives $N_1^{ph} - N_0^{ph} \sim 2.33$. We are thus facing a totally different physical picture: the excited state is composed of a polaron which contains several extra phonon excitations (in comparison to the ground-state polaron) and the binding energy of the excited polaron is $\Delta<0$. The extra phonon excitations are located almost entirely on the electron site [see the inset of Fig. 10(d)]. The value of $\gamma_1 - \gamma_0$ at $j=0$ is 2.16, which almost exhausts the phonon sum.

B. Strong-coupling perturbation theory

In this section we calculate the ground- and excited-state energies of the polaron perturbatively in the hopping t. For $t=0$, the Hamiltonian Eq. (1) describes a harmonic oscillator with a shifted origin (due to the λ force term) on the site with the electron, and unshifted oscillators on the other sites. The Hamiltonian in the new basis is given by the canonical transformation $\tilde{H}=e^S H e^{-S}$, where

$$S=-g\sum_j n_j(a_j-a_j^\dagger), \qquad (8)$$

and $g=\lambda/\omega$.[32] After some algebra (see also Ref. 12), the transformed Hamiltonian takes the following form:

$$\tilde{H}=H_0+V, \quad H_0=\omega\sum_j a_j^\dagger a_j - \omega g^2 \sum_j n_j,$$

$$V=-te^{-g^2}\sum_j (c_j^\dagger c_{j+1} e^{g(a_j^\dagger - a_{j+1}^\dagger)} e^{-g(a_j - a_{j+1})} + \text{H.c.}),$$

$$(9)$$

where $n_j=c_j^\dagger c_j$. The operator $a_j^\dagger$ in Eq. (9) creates a phonon excitation on site j relative to the shifted oscillator if there is an electron on site j, and relative to an unshifted oscillator on the other sites. The first term in H_0 is the energy of the phonon excitations, and the second is the energy gained by the oscillator that is displaced by the force of the electron. In strong-coupling perturbation theory, V in Eq. (9) is considered a perturbation. It represents the hopping of an electron, including possible creation and destruction of phonon excitations.

The lowest energy eigenstates of the unperturbed Hamiltonian H_0 have no extra phonon excitations, and an energy $E_0^{(0)}=-\lambda^2/\omega$. They can be written $|\phi_0(j)\rangle=c_j^\dagger|\mathcal{O}\rangle$, where $|\mathcal{O}\rangle$ represents vacuum for electron and phonon degrees of freedom. This state represents a polaron localized on the site j. Evidently the ground state is N-fold degenerate, where N is the number of sites in the system. The perturbation lifts this degeneracy. The matrix elements $V_0(i,j)=\langle\phi_0(i)|V|\phi_0(j)\rangle$ can be readily computed since the exponential factors in V are not effective in this case,

$$V_0(i,j)=-te^{-g^2}, \quad j=i\pm 1. \qquad (10)$$

This describes a translation-invariant tight-binding model in one dimension with nearest-neighbor hopping. To first order in t, the ground-state energy of a polaron with momentum k is

$$E_0(k)=-\lambda^2/\omega - 2te^{-g^2}\cos k. \qquad (11)$$

Excited states. The lowest energy states of H_0 are the N degenerate states of energy $-\lambda^2/\omega$, considered above. The next lowest energy sector contains the N^2 degenerate states of energy $-\lambda^2/\omega+\omega$, of the form $|\psi_1(j,l)\rangle=c_j^\dagger a_l^\dagger|\mathcal{O}\rangle$. The electron is on site j and the additional phonon excitation is on site l. We do degenerate perturbation theory to $O(t)$ in this excited sector. Using the total momentum k as a good quantum number, the 2D tight-binding problem in (j,l) becomes a 1D tight-binding problem. The 1D basis functions are $|\phi_1(j)\rangle=|\psi_1(0,j)\rangle$, where j is the distance between the phonon and the electron. The nonzero matrix elements $V_1(i,j)=\langle\phi_1(i)|V|\phi_1(j)\rangle$ are

$$V_1(0,0)=-2tg^2 e^{-g^2}\cos k,$$

$$V_1(0,\pm 1)=-t(1-g^2)e^{-g^2},$$

$$V_1(-1,1)=-tg^2 e^{-g^2}e^{ik}, \quad V_1(i,j)=-te^{-g^2},$$

$$j=i\pm 1, \quad i,j\neq 0. \qquad (12)$$

This is a 1D tight-binding model that is translation-invariant except near the origin, where there is a second-neighbor hopping term and other modifications. The matrix $V_1(i,j)$ is Hermitian. Matrix elements in Eq. (12) define a secular equation $|V(k)-E(k)|=0$ for the energies that can easily be solved numerically for a large system. For each total wave vector k, there are N-independent solutions. The lowest energy first excited state at momentum k is

$$E_1(k)=-\lambda^2/\omega+\omega+E_1^{(1)}(k), \qquad (13)$$

where $E_1^{(1)}(k)$ is the lowest energy solution of the secular equation.

The numerical and analytic solution of the secular equation reveals that there is a true phase transition (energy nonanalytic in the parameters) for the first excited state. This is perhaps surprising in light of the theorem that there can be no phase transition for the ground state,[24] and demonstrates the impossibility of extending the theorem to include excited states. We consider first a total momentum $k=0$. For $g>g_1=1$, the lowest energy first excited state is found to be a bound state of a polaron and an additional phonon. The bound state is Raman active. For $g<g_1$, the first excited state is unbound, with an energy exactly ω higher than the ground state. This energy is in fact an upper bound for the first excited state in any dimension and at any $\vec{k}$, since one can construct a variational state with a zero momentum polaron and a momentum $\vec{k}$ phonon at infinite separation. The energy of the first excited state is nonanalytic (discontinuous first derivative) at $g=g_1$. The bound-state formation is unusual for several (related) reasons: (a) For $g>g_1$, the binding energy is linear in $(g-g_1)$ for small $(g-g_1)$, rather than the $(g-g_1)^2$ dependence that is typical for 1D bound-state problems. (b) For $g<g_1$, the phase shift is zero between the polaron and an additional unbound phonon of relative momentum $q\to0$. The polaron and additional phonon pass through each other transparently, in contrast to the usual repulsive phase shift. (c) At $g=g_1$, even for finite N (periodic boundary conditions), there are two exactly degenerate ground states, in contrast to the usual avoided crossing. These unexpected properties result in part from the fact that the central site in the tight-binding model [Eq. (12)] becomes uncoupled from the rest of the lattice precisely at $g=g_1$. The binding energy in 1D can, in fact, be determined analytically from Eq. (12). One can show that for $g\geq g_1$, $E_1^{(1)}(k)=-te^{-g^2}(x^2+1)/x$, where

$$x=\frac{3g^2-1+\sqrt{(9g^2-1)(g^2-1)}}{2}, \quad k=0,$$

$$x=g^2, \quad k=\pi. \quad (14)$$

The $O(t)$ strong-coupling analysis can be extended to higher dimensions and to nonzero total momentum $\vec{k}$. The $\vec{k}=0$ state always has an energy less than or equal to that at any other $\vec{k}$. We find that for $g<g_1$, the first excited state at any momentum $\vec{k}$ is unbound, with $g_1=1$ in any dimension $d\geq1$. The $k=0$ phase shift also vanishes for $g<g_1$ in any dimension. For $g>g_2$, the first excited state at any momentum is bound.[33] For $g_1<g<g_2$, there is a phase transition on a surface in $\vec{k}$ space such that inside the surface (including $\vec{k}=0$) the first excited state is bound, and outside the surface [including $\vec{k}=(\pi,\pi,\dots)$] the first excited state is unbound. The location of the surface in $\vec{k}$ space is g dependent. The numerically obtained values are $g_2=2.1$ in 3D, $g_2=1.66$ in 2D, and $g_2=g_1=1$ in 1D. [1D is special in that there is no intermediate phase. However, as $g\to g_1^+$ in 1D, the $k=\pi$ state is very weakly bound compared to $k=0$; see Eq. (14). The $k=\pi$ state has zero amplitude to have the electron and

the additional phonon on the same site.] The binding energy at $\vec{k}=0$ is linear in $(g-g_1)$ for higher dimensions, as it is in 1D.

Strong-coupling perturbation theory is carried to $O(t^2)$ in the Appendix.

V. CONCLUSIONS

In summary, we have presented a variational approach for solving the Holstein model with dynamical, quantum phonons based on an exact diagonalization method. The variational space is defined on an infinite lattice. It is constructed by successive application of the off-diagonal terms of the Hamiltonian starting from a single-electron state. This leads to a systematically improvable variational basis that turns out to be efficient for calculating the ground-state and low-lying excited-state properties of the model. The method can compute properties in all parameter regimes, but it is at its best in the intermediate-coupling regime, where strong- and weak-coupling perturbation theories and other variational methods have problems.

The method allows the computation of energy bands and other physical properties at continuous wave vectors. For intermediate-coupling strengths we are able to reach an accuracy of 12 digits for the ground-state energy at small k with as few as $M=88\,052$ basis states and only a few seconds of CPU time on a workstation. Our results for energy bands presented in Fig. 3 compare well with other numerically more intensive methods and are more precise at both large and small k than some of them. Our energies are variational in the thermodynamic limit for any k. We believe that all results shown for energy bands computed with $M=3\times10^6$ states converge to at least four digits for arbitrary k.

The accuracy of our method can be seen from the comparison of effective masses in Fig. 4. While our results have converged to at least four digits in all parameter regimes presented in Fig. 4, GL and DMRG methods give less reliable results. While deviations of DMRG are insignificant, deviations of GL results near strong coupling seem to be systematic. Results for the quasiparticle residue as a function of the wave vector in the weak-coupling regime show a smooth crossover between the predominantly electronic character to a predominantly phononic character of the polaron. Our results agree with previous ED calculations.

The correlation functions χ agree well with DMRG results in the intermediate-coupling regime. In the weak-coupling regime our method gives more reliable results. Close to the extreme strong-coupling and adiabatic regime, our correlation functions have not fully converged as a function of N_h for $N_h=21$, $M=6\times10^6$. Our results in this regime are qualitatively similar to, but less accurate than, those of the DMRG. Correlation functions χ computed at different k provide detailed information on how the weak-coupling polaron transforms as k increases from $k=0$ to $k=\pi$.

Using numerical and strong-coupling approaches, we find a true phase transition (rather than a crossover) in the first excited state, where a polaron plus phonon system changes from unbound at weak coupling to bound at strong coupling. The first excited state does not contribute to the optical conductivity, but rather is Raman active.

There are a number of extensions to this work that we

have not included in this paper. It is straightforward to consider anharmonic phonons. (In fact, the extreme double-well limit where only the lowest two states are retained is numerically less demanding than the linear case.) The ac conductivity and spectral function of a polaron can be calculated by the same methods. Properties of other Hamiltonians, including those with SSH-type couplings where phonons modify the hopping t can be calculated. Extensions that allow certain phonon excitations to be infinitely far from the electron are possible. Properties in higher spatial dimensions can be calculated. One can also calculate the properties of bipolarons, including Hubbard on-site and longer-range interactions between electrons. And finally, one can calculate the coherent quantum dynamics of electron-phonon coupled systems driven far from equilibrium using similar methods.[19,20]

APPENDIX

For simplicity we have limited our calculation of the energy corrections in second-order strong-coupling perturbation theory to 1D and zero momentum, $k=0$. Following the work of Marsiglio,[12] the ground-state correction to second order in the hopping t is given by

$$E_0^{(2)} = -2t^2 \frac{e^{-2g^2}}{\omega} \left[\sum_{n,m=1} \frac{g^{2(m+n)}}{n!m!} \frac{1}{n+m} + 3 \sum_{n=1} \frac{g^{2n}}{n!} \frac{1}{n} \right]. \tag{A1}$$

Calculation of the energy corrections of the excited-state energy E_1 involves degenerate perturbation theory, where matrix elements between degenerate states $|\phi_1(j)\rangle$ are computed to second order in t. After a straightforward but tedious calculation we obtain for the nonzero matrix elements

$$V_1(0,0) = -2tg^2 e^{-g^2}$$
$$+ 2t^2 \frac{g^2 e^{-2g^2}}{\omega} \left[\sum_{n,m=1} \frac{g^{2(m+n)}}{n!m!} \frac{\left(1-\frac{n}{g^2}\right)^2}{1-n-m} \right.$$
$$\left. + \sum_{n=2} \frac{g^{2n}}{n!} \frac{\left(1-\frac{n}{g^2}\right)^2 + 2}{1-n} + 2 \right], \tag{A2}$$

$$V_1(0,1) = -t(1-g^2)e^{-g^2}$$
$$- t^2 \frac{g^2 e^{-2g^2}}{\omega} \left[\sum_{n,m=1} \frac{g^{2(m+n)}}{n!m!} \frac{\left(1-\frac{n}{g^2}\right)\left(1-\frac{m}{g^2}\right)}{1-n-m} \right.$$
$$\left. + 3 \sum_{n=2} \frac{g^{2n}}{n!} \frac{\left(1-\frac{n}{g^2}\right)}{1-n} + 2 \right], \tag{A3}$$

$$V_1(1,1) = t^2 \frac{e^{-2g^2}}{\omega} \left[\sum_{n,m=1} \frac{g^{2(m+n)}}{n!m!} \left(\frac{g^2\left(1-\frac{n}{g^2}\right)^2}{1-n-m} - \frac{1}{n+m} \right) \right.$$
$$\left. + \sum_{n=2} \frac{g^{2n}}{n!} \frac{2g^2-2n+\frac{n}{g^2}(n+2)}{1-n} + g^2 \right], \tag{A4}$$

$$V_1(-1,1) = -tg^2 e^{-g^2} + t^2 \frac{g^2 e^{-2g^2}}{\omega}$$
$$\times \left[\sum_{n=2} \frac{g^{2n}}{n!} \frac{\left(1-\frac{n}{g^2}\right)^2}{1-n} + 1 \right], \tag{A5}$$

$$V_1(0,2) = -t^2(1-g^2) \frac{e^{-2g^2}}{\omega} \sum_{n=1} \frac{g^{2n}}{n!} \frac{1}{n}, \tag{A6}$$

$$V_1(j,j+2) = -t^2 \frac{e^{-2g^2}}{\omega} \sum_{n=1} \frac{g^{2n}}{n!} \frac{1}{n}, \quad j \geq 1 \tag{A7}$$

$$V_1(j,j) = -2t^2 \frac{e^{-2g^2}}{\omega} \left[\sum_{n,m=1} \frac{g^{2(m+n)}}{n!m!} \frac{1}{n+m} \right.$$
$$\left. + 2 \sum_{n=1} \frac{g^{2n}}{n!} \frac{1}{n} \right], \quad j \geq 2 \tag{A8}$$

$$V_1(j,j+1) = -te^{-g^2}, \quad j \geq 1. \tag{A9}$$

For $k=0$, $V_1(i,j) = V_1(j,i) = V_1(-i,-j)$. We numerically solve the secular equation $|V-E| = 0$. The lowest eigenvalue $E_1^{(1,2)}$ of the secular equation gives us corrections to the excited-state energy E_1 to second order in the hopping t,

$$E_1 = -\lambda^2/\omega + \omega + E_1^{(1,2)}. \tag{A10}$$

The binding energy to second order at $k=0$ is given by Eqs. (11), (A1), and (A10),

$$\Delta = E_1^{(1,2)} + 2te^{-g^2} - E_0^{(2)}. \tag{A11}$$

The second-order results are used to calculate the phase boundary in Fig. 9.

[1] M. Jaime, H.T. Hardner, M.B. Salamon, M. Rubinstein, P. Dorsey, and D. Emin, Phys. Rev. Lett. **78**, 951 (1997).

[2] A.P. Ramirez, J. Phys.: Condens. Matter **9**, 8171 (1997).

[3] *Lattice Effects in High-T_c Superconductors*, edited by Y. Bar-Yam, T. Egami, J. Mustre de Leon, and A. R. Bishop (World Scientific, Singapore, 1992).

[4] A.S. Alexandrov and N.F. Mott, Rep. Prog. Phys. **57**, 1197 (1994).

[5] A.S. Alexandrov and N.F. Mott, *Polarons and Bipolarons* (World Scientific, Singapore, 1995).

[6] A.S. Alexandrov, V.V. Kabanov, and D.E. Ray, Phys. Rev. B **49**, 9915 (1994).

[7] G. Wellein, H. Röder, and H. Fehske, Phys. Rev. B **53**, 9666 (1996).

[8] G. Wellein and H. Fehske, Phys. Rev. B **56**, 4513 (1997).

[9] G. Wellein and H. Fehske, Phys. Rev. B **58**, 6208 (1998).

[10] E.V.L. de Mello and J. Ranninger, Phys. Rev. B **55**, 14 872 (1997).

[11] M. Capone, W. Stephan, and M. Grilli, Phys. Rev. B **56**, 4484 (1997).

[12] F. Marsiglio, Physica C **244**, 21 (1995).

[13] H. De Raedt and A. Langedijk, Phys. Rev. Lett. **49**, 1522 (1982); Phys. Rev. B **27**, 6097 (1983); **30**, 1671 (1984).

[14] P.E. Kornilovitch and E.R. Pike, Phys. Rev. B **55**, R8634 (1997).

[15] A.W. Romero, D.W. Brown, and K. Lindenberg, J. Chem. Phys. **109**, 6540 (1998).

[16] A.W. Romero, D.W. Brown, and K. Lindenberg, cond-mat/9806032 (unpublished).

[17] E. Jeckelmann and S.R. White, Phys. Rev. B **57**, 6376 (1998).

[18] E. Jeckelmann (private communication).

[19] J. Bonča and S.A. Trugman, Phys. Rev. Lett. **79**, 4874 (1997).

[20] J. Bonča and S.A. Trugman, Phys. Rev. Lett. **75**, 2566 (1995);

[21] E.V. Anda, S.S. Makler, H.M. Pastawski, and R.G. Barrera, Braz. J. Phys. **24**, 330 (1994).

[22] G. D. Mahan, *Many-Particle Physics* (Plenum, New York, 1981).

[23] A.J. Leggett, S. Chakravarty, A.T. Dorsey, M.P.A. Fisher, A. Garg, and W. Zwerger, Rev. Mod. Phys. **59**, 1 (1987).

[24] T. Holstein, Ann. Phys. (N.Y.) **8**, 325 (1959).

[25] B. Gerlach and H. Lowen, Rev. Mod. Phys. **63**, 63 (1991).

[26] It is possible to construct a variational space with a different tradeoff between phonon number and phonon distance. It is sometimes useful at very strong coupling to add to the Hilbert space states with a very large number of phonon quanta on the electron site.

[27] S. A. Trugman, in *Applications of Statistical and Field Theory Methods to Condensed Matter*, edited by D. Baeriswyl, A.R. Bishop, and J. Carmelo (Plenum Press, New York, 1990).

[28] A.A. Gogolin, Phys. Status Solidi B **109**, 95 (1982).

[29] We thank H. Fehske for providing these unpublished ED results. The $\lambda/\omega = 1$ results are for 16 sites, 10 phonons, with 5.3×10^6 basis states in the symmetrized Hamiltonian. The $\lambda/\omega = \sqrt{2}$ results are for 16 sites, 12 phonons (3.0×10^7 basis states). These ED results are quite accurate, although we believe that we obtain 5 significant figures greater accuracy with a Hilbert space that is 50 times smaller.

[29] H. Sumi, J. Phys. Soc. Jpn. **36**, 770 (1974).

[30] S. Ciuchi, F. de Pasquale, S. Fratini, and D. Feinberg, Phys. Rev. B **56**, 4494 (1997).

[31] H. Fehske (private communication).

[32] I.G. Lang and Yu.A. Firsov, Zh. Éksp. Teor. Fiz. **43**, 1843 (1962) [Sov. Phys. JETP **16**, 1301 (1963)]; Fiz. Tverd. Tela (Leningrad) **5**, 2799 (1966) [Sov. Phys. Solid State **5**, 2049 (1964)].

[33] The first excited state at nonzero momentum $\vec{k}$ is a bound state if $E_1(\vec{k}) - E_0(\vec{k}=0) < \omega$, so that decay into a polaron and a phonon is energetically forbidden.